Supplementary Materials for: Diverse environmental perturbations reveal the evolution and context-dependency of genetic effects on gene expression levels

Amanda J. Lea[1,2,3*], Julie Peng[1,2], Julien F. Ayroles[1,2*]

1. Department of Ecology and Evolution, Princeton University, Princeton, New Jersey, USA
2. Lewis Sigler Institute for Integrative Genomics, Princeton University, Princeton, New Jersey, USA
3. Present address: Department of Biological Sciences, Vanderbilt University, Nashville, Tennessee, USA

*Correspondence to: amanda.j.lea@vanderbilt.edu, jayroles@princeton.edu

The PDF file includes:
Supplementary Methods
Supplementary Figures
Supplementary References

SUPPLEMENTARY METHODS

Cells and cell culture prior to experimental treatments

Lymphoblastoid cell lines (LCLs) were obtained for 544 unrelated individuals included in the 1000 Genomes study (The 1000 Genomes Project Consortium 2012). All cells were ordered from Coriell Institute, and a complete list of the included lines is available in Table S1. Live cultures were shipped overnight to Princeton University in randomized batches of 25 (Table S1). Two batches of 25 were shipped on Monday and Tuesday of a given week and processed in parallel over the following two weeks; after the two-week period, another two batches of 25 arrived (and so on).

Upon arrival of a given batch of 25 samples, cells were incubated overnight in the flasks they were shipped in (unopened) at 37°C with 5% CO2. On day 2, cells were pelleted, counted using Trypan blue stain and a Countess Automated Cell Counter, and resuspended at a density of 500,000 cells per mL of cell culture media (RPMI + 10% fetal bovine serum + 1% antibiotic). Cells were then checked and split every 48 hours until a total of 14 million cells (12 million for our experiments and 2 million for cryopreservation) were obtained for a given line, or until 11 days had passed, whichever came first. At this time, we seeded 1 million cells in 2.5mL of media in each well of a 12 well plate, using one plate per individual. In cases where we had <12 million cells on the day of seeding, we plated however many wells we could. The 12 well plates were then placed overnight in an incubator and experimental treatments were performed on the morning of the following day (see below).

We note that cells were not starved of serum prior to treatment. This is sometimes done to synchronize all cells to the same cell cycle phase and/or to eliminate any potential effects of fetal bovine serum on cellular responses (because serum contains many small molecules and proteins and is not well-defined between lots and manufacturers (Zheng et al. 2006)). However, the practice of cell starvation can affect cell viability and morphology (Rashid and Coombs 2019), and we therefore did not include it in our experimental design. We also note that, while it was infeasible to use the same lot of serum across the entire experiment, the same lot of serum was used to culture all cells from a given individual. Therefore, between-lot differences in serum composition would not affect any inferences about within-individual responses. Further, the between-individual variables of interest in our study are genotype and ancestry, which were completely randomized across cell growth batches (and consequently across serum lots).

Cell treatments

On the morning of the experiment, a given 12 well plate was removed from the incubator and 5 ul of each treatment was added to a predesignated well. Table S2 shows the concentrations used for each of the experimental treatments. These concentrations were derived from the literature and modified in some cases based on pilot experiments. We note that our goal here was to learn about the general properties of genotype x environment interactions, rather than to create a realistic cellular model for any individual treatment; thus, in some cases we chose concentrations that provoked a gene expression response in our pilot experiments rather than concentrations that were physiologically realistic. Because our treatments were dissolved in either water or ethanol, we also included these two molecules as controls, for a total of 12 conditions. We did not monitor cell viability, but based on previous work we believed that the concentration of ethanol we used would not have effects toxicity effects. In particular, previous work in a variety of cell types has shown that toxicity effects begin at concentrations of ~5%

(Nguyen et al. 2020) and this manifests most strongly at time periods greater than 24 hours (Tuoi Do et al. 2011). At concentrations similar to ours (<1%), ethanol does not appear to affect cell viability or growth (Casañas-Sánchez et al. 2016; Šarc and Lipnik-Štangelj 2009).

Following the addition of all 12 treatment and control molecules, plates were returned to the incubator for 4 hours, after which we spun down the plates for 5 min at 500 g at 4C. We then removed the cell culture media and washed the cells twice in cold 1x phosphate-buffered saline, spinning each wash for 10 min at 500 g at 4C. Finally, we lysed cells in 400 ul of a homemade lysis buffer that was made with the following recipe: 100 mM Tris-HCl at pH 7.5, 500 mM LiCl, 10 mM EDTA at pH 8, 1% LiDS, 5 mM dithiothreitol (DTT), and 10% beta mercaptoethanol. All lysed cells were then frozen at -80C.

RNA extraction and library preparation

12 well plates were thawed in batches of 8 or 12, depending on whether we were performing RNA extractions for all 12 conditions or just for 8 conditions (which we did for a subset of individuals). Depending on the circumstances, 12 conditions from 8 cell lines or 8 conditions from 12 cell lines were plated on a 96-well plate, with 3 wells randomly left empty as negative controls. To avoid introducing new batch effects, the samples that were plated together on a given 96-well plate were randomly chosen from a given batch of 50 samples that were received and processed during the same two-week period.

We used 200 ul of each sample to extract RNA using Zymo's Quick-RNA 96 kit, following the manufacturer's instructions. RNA extractions were repeated for a given plate if there was evidence of contamination in the negative control wells. mRNA-seq libraries were prepared using the published TM3'seq protocol (Pallares et al. 2020) and a CyBio FeliX liquid handling robot (Analitik Jena). After the final PCR step, 5 ul of each library derived from a given cell line (n=8 or 12) were pooled, cleaned using SPRI beads, and quantified with a Qubit fluorimeter. The line level pools were then equimolarly combined into a plate level pool, which was visualized and quantified on an Agilent TapeStation. The total dataset (n=5223 libraries) was sequenced across four runs of the Illumina NovaSeq platform. Each sample was sequenced to a mean depth of 2.199 ± 2.731 (SD) million reads using 100bp single end sequencing.

Low level RNA-seq data processing

Each sample was trimmed for low quality bases and adapter contamination using cutadapt (Martin 2011). Trimmed reads were then mapped to the human reference genome (hg38) using STAR (Dobin et al. 2013) and filtered for unique mapping. We checked for potential ancestry biases in mapability, by asking whether the proportion of reads that uniquely map (relative to the total number of reads generated) differed by ancestry and found that this was generally not the case. For example, analyzing all samples within one of our sequencing batches (n=1344 samples) and using the CEU/CEPH population as the reference, we found that only GWD had a significantly lower mapping rate (linear model, beta=-1.96, p=0.0073; Figure S5).

Using our set of uniquely mapped reads, we counted the number of reads that overlapped each gene using HTSeq (Anders 2011) and the GENCODE v25 GTF (https://www.gencodegenes.org/human/release_25.html). If a sample had fewer than 250,000 reads mapped to protein coding genes, we excluded it from further analyses. This filtering step left us with 3886 samples and the metadata for these samples is provided in Table S3. Matrices of read counts per filtered sample were assembled and exported for further processing.

We translated our raw count data into transcripts per million (TPM), and filtered the dataset to exclude non-protein coding genes as well as genes that were lowly expressed in all conditions (median TPM<2 in all 12 conditions). This left us with 10157 genes for analysis. Next, we used the voom function in the R package limma (Law et al. 2014) to normalize the count data. To remove variance attributed to batch and other technical effects, we conducted surrogate variable analysis (Leek and Storey 2009) on the voom-normalized data (protecting the variance associated with treatment (12-way factor) and population (AFR/EUR)). We then fit linear models in limma (Law et al. 2014) and regressed out three surrogate variables, the number recommended by the num.sv function. As expected, the three surrogate variables were highly correlated with the first 3 principal components of the normalized gene expression matrix (Pearson correlation R=-0.944, -0.929, and 0.819, all $p<10^{-16}$). They were also correlated with known technical effects such as total read depth (R between SV1 and SV2 and total read depth=-0.319 and 0.131, both $p<10^{-16}$) and sequencing batch (ANOVA of SV2 and sequencing batch: F=109.47, $p<10^{-16}$). Importantly, because cell lines were randomized across all batch effects within the experiment, there should be no confounds between batch effects and our variables of interest. Principal components analyses of the SV-corrected dataset are presented in Figure S6.

Low level genotype data processing

We downloaded phased genotype calls, derived from ~30× whole genome sequence data, for 454 1000 Genomes Project individuals included in our study (Byrska-Bishop et al. 2021) (Table S4). We the used PLINK (Purcell et al. 2007) to remove the following variant types: indels, SNPs with >2 alleles, SNPs with MAF<0.05, SNPs called in <50% of individuals, and SNPs out of Hardy-Weinberg equilibrium ($p<10^{-6}$). This filtering left us with 7,205,828 SNPs. We then performed LD filtering using the indep-pairwise command in PLINK (Purcell et al. 2007), with a window size of 500kb, a step size of 50kb, and an R^2 threshold of 0.8. We used these LD-filtered SNPs to generate a PCA in PLINK (Purcell et al. 2007) as well as a genetic relatedness matrix (GRM) in GCTA (Yang et al. 2011). Finally, to prepare for cis eQTL mapping, we extracted 1,950,183 LD-filtered SNPs that fell within 500kb of the transcription start or end site of protein coding genes.

Understanding the effects of sequence coverage

Some of our mRNA-seq libraries were sequenced at relatively low coverage. This is appropriate for the 3' biased approach that we used (Pallares et al. 2020), but could still impact our ability to identify genetic, ancestry, or treatment effects on gene expression, especially for lowly expressed genes. To understand how sequence coverage impacts our results and main conclusions, we performed two analyses. First, we compared the log fold changes we see in this study in response to Dexamethasone to another study that used the same cell type and concentration and a full transcript/higher sequencing coverage approach (Moyerbrailean et al. 2016). We note that such a comparison is not possible for all treatments, because we do not know of other publicly available datasets that used our exact parameters. For the Dexamethasone comparison, we estimate extremely similar effect sizes relative to previous work (Pearson correlation=0.73, $p<10^{-16}$; Figure S9).

Second, we repeated our analyses of ancestry and treatment effects after splitting our samples into two datasets: one dataset that contained the samples with the highest read coverages and one dataset that contained the samples with the lowest read coverages. We then reran our analysis pipeline and compared the results. When we analyzed samples from the lower and upper

half of coverages, we estimated extremely similar ancestry and treatment effects: the mean Pearson correlation for ancestry and treatment effect sizes estimated in the two datasets was 0.80 ± 0.01 and 0.50 ± 0.20, respectively (both $p<10^{-16}$). This is not to say that coverage has no impact on the effect sizes we can detect, *it will in any dataset.* However, we have found that the effect sizes we estimate are robust and similar to previous studies as well as our own dataset divided by coverage.

Estimating the heritability of gene expression levels

We used GCTA and the GRM derived from the dataset of filtered genotypes to estimate the heritability of gene expression levels in each cellular environment. We followed the pipeline recommended by the authors (https://cnsgenomics.com/software/gcta/#GREMLanalysis) and estimated heritability for each of 10,156 genes in each of the 12 cellular environments. We note that, given our sample sizes, per-gene heritability estimates are noisy and future studies with larger sample sizes will be needed to obtain more accurate gene-specific values in a given cellular environment (Visscher et al. 2014). Instead, our goal here was to understand whether the overall heritability distributions changed as a function of the cellular environment. To do so, we used a Wilcoxon signed-rank test to ask whether mean heritability differed between each treatment-control pair (see Figure 3 and Table S5). Because we observed upward biases in heritability estimates for conditions with the smallest sample sizes, we also 1) repeated the same analysis after subsampling each environment to n=100 individuals (performing 5 independent subsamples) and 2) used linear models to ask whether there was a consistent difference in per-gene heritability estimates between treatment and control conditions controlling for sample size.

Enrichment analyses of treatment- and ancestry-associated genes

We used gene set enrichment analyses (GSEA) (Subramanian et al. 2005) to ask whether certain biological pathways were overrepresented among the set of genes that exhibited the strongest evidence for 1) differential expression in response to a given treatment and 2) ancestry-associated differences in expression. For #1, we sorted our gene list by effect size (output from limma) for each treatment effect separately and ran GSEA. For #2, we sorted our gene list by median effect size across all conditions, because very few genes exhibiting evidence for ancestry effect size heterogeneity across conditions. We assessed the significance of pathway enrichment scores via comparison to 1000 random permutations of gene labels across pathways, and controlled for multiple hypothesis testing using a Storey-Tibshirani FDR approach (Storey and Tibshirani 2003). Results are reported in Figure S1, Tables S6, and Table S9.

We also tested whether ancestry-associated genes shared between ≥2/3 of all conditions (as determined by mashR (Urbut et al. 2019)) were enriched within genes associated with 114 complex traits and diseases. To do so, we followed the approach of (Findley et al. 2021) and drew on publicly available results from Probabilistic Transcriptome Wide Association Studies (PTWAS) (Zhang et al. 2020). PTWAS combines eQTL data from GTEx (Aguet et al. 2017) and GWAS data from several studies to identify genes that are likely along the causal pathway for a given complex trait or disease. We used hypergeometric tests to test for enrichment of ancestry-associated genes within each PTWAS trait-associated gene set and an FDR approach (Storey and Tibshirani 2003) to correct for multiple hypothesis testing. Results are reported in Table S10.

Enrichment analyses of ubiquitous and context-dependent eQTL and eGenes

We performed several enrichment analyses to understand the biology and putative phenotypic impacts of SNPs and genes that exhibited ubiquitous (shared across all 12 conditions) and context-dependent (condition-specific or shared across 2-11 conditions) eQTL.

First, to investigate the cellular mechanisms involved in generating ubiquitous and context-dependent eQTL, we downloaded ATAC-seq data generated for 20 LCLs from Yoruba 1000 Genomes individuals (Banovich et al. 2018). These data were preprocessed and provided as count matrices noting the number of reads mapped to a given region (n=2,533,845 windows) for a given individual. To identify strong and repeatable regions of open chromatin, we normalized the count matrix using the function voom in the R package limma (Law et al. 2014); we then retained regions for which the average normalized read counts were in the upper quartile of the entire dataset, and lifted over the region coordinates from hg19 to hg38 using the UCSC liftOver tool (Karolchik et al. 2014). Finally, we used BEDTools (Quinlan and Hall 2010) to calculate the proportion of ubiquitous and context-dependent eQTL that overlapped with LCL ATAC-seq peaks, and we compared these proportions to background expectations derived from counting the proportion of all tested SNPs that overlapped with LCL ATAC-seq peaks. We performed these analyses using hypergeometric tests.

Second, we asked whether ubiquitous or context-dependent eQTL were enriched in particular chromatin states as annotated by ENCODE for GM12878 LCLs (The ENCODE Project Consortium 2012). To do so, we downloaded publicly available ChromHMM annotations for this cell type from: http://hgdownload.cse.ucsc.edu/goldenPath/hg19/encodeDCC/wgEncodeBroadHmm/. We then used Fisher's exact tests to evaluate whether each group of eQTL (ubiquitous or context-dependent) was enriched in a given chromatin state relative to all SNPs tested as putative eQTL.

Third, we asked whether ubiquitous or context-dependent eQTL genes were enriched within the set of eGenes identified in unstimulated LCLs by GTEx (Aguet et al. 2017) (i.e., genes with at least 1 eQTL identified at a 10% FDR). To do so, we used hypergeometric tests to compare our list of ubiquitous or context-dependent eGenes to GTEx eGenes, after first filtering for expressed genes that were common to both datasets. We also used hypergeometric tests to ask whether context-dependent eGenes that were not identified as eGenes in GTEx, but were identified as eGenes in our study, were enriched for genes that were also differentially expressed in our study (suggesting that cell perturbations "reveal" new eQTL). For this analysis, we used a combined list of all genes that were differentially expressed in any condition (FDR<10% from the limma output).

Third, we asked whether ubiquitous or context-dependent eGenes were enriched within sets of genes associated with 114 complex traits and diseases via PTWAS (Zhang et al. 2020). Here, we performed separate hypergeometric tests for each complex trait and each eGene list, and corrected for multiple hypothesis testing with a Storey-Tibshirani FDR approach (Storey and Tibshirani 2003).

Fourth, we downloaded the list of genes that are considered to be loss of function, mutation-intolerant genes, as curated by ExAC (Lek et al. 2016). We then used Fisher's exact tests and asked whether ubiquitous or context-dependent eQTL genes were enriched within the total set of mutation-intolerant genes.

Fifth, we downloaded the GWAS catalog (Hindorff et al. 2009) and filtered for SNPs with $p<10^{-8}$. We then used Fisher's exact tests to ask whether ubiquitous or context-dependent eQTL loci were enriched within the GWAS catalog.

SUPPLEMENTARY FIGURES

Figure S1. Gene set enrichment analyses reveal changes in expected gene categories. Results from gene set enrichment analyses testing for overrepresentation of particular Gene Ontology categories among differentially expressed genes in response to A) Tunicamycin, B) IFNG, C) Gardiquimod, and D) B cell activating factor. We focus on these 4 environmental treatments as quality control, because we have relatively strong expectations for which biological pathways they should affect. In all cases, only the top 15 most significant categories are shown. Enrichment maps were created with the emapplot function in the R package enrichplot.

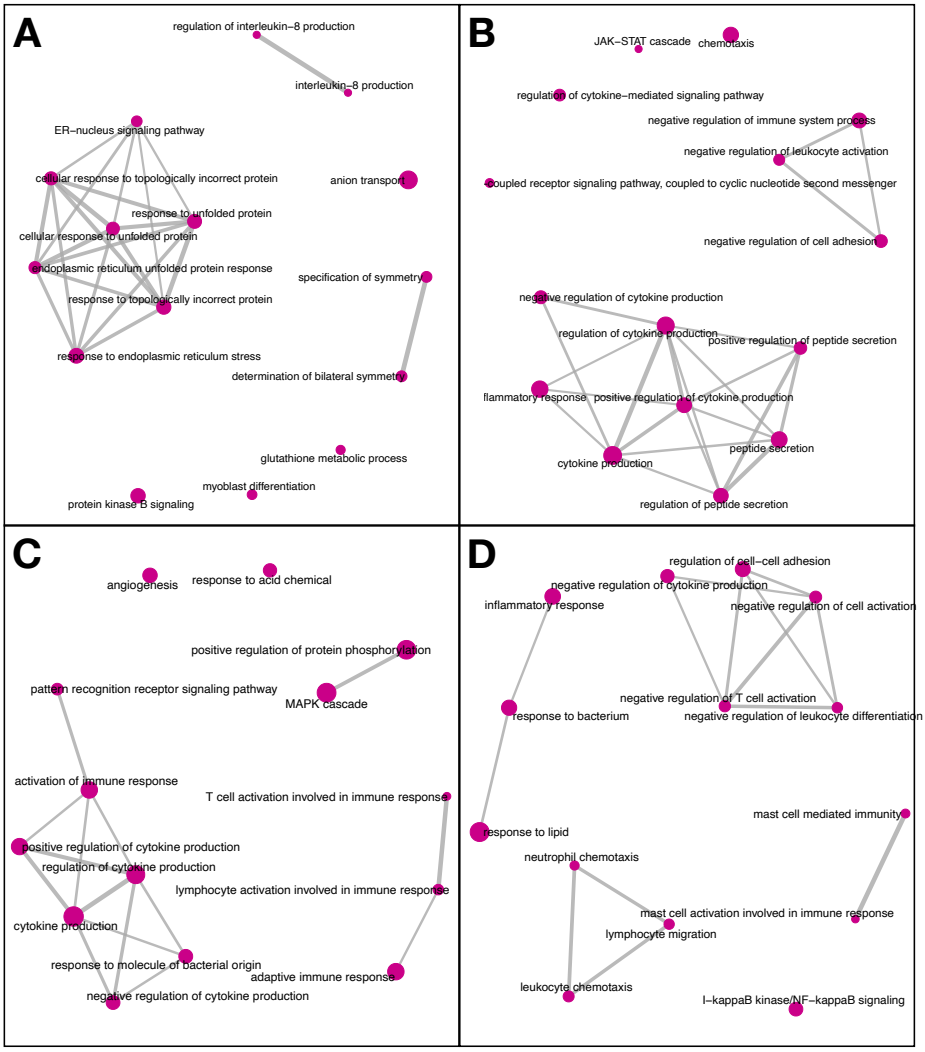

Figure S2. Sharing of environmental and ancestry effects on gene expression levels. Plots show the degree of correlation between the mashR (Urbut et al. 2019) posterior mean estimates for (A) differentially expressed genes in response to a given environmental treatment and (B) differentially expressed genes as a function of ancestry (African versus European) in a a given cellular environment.

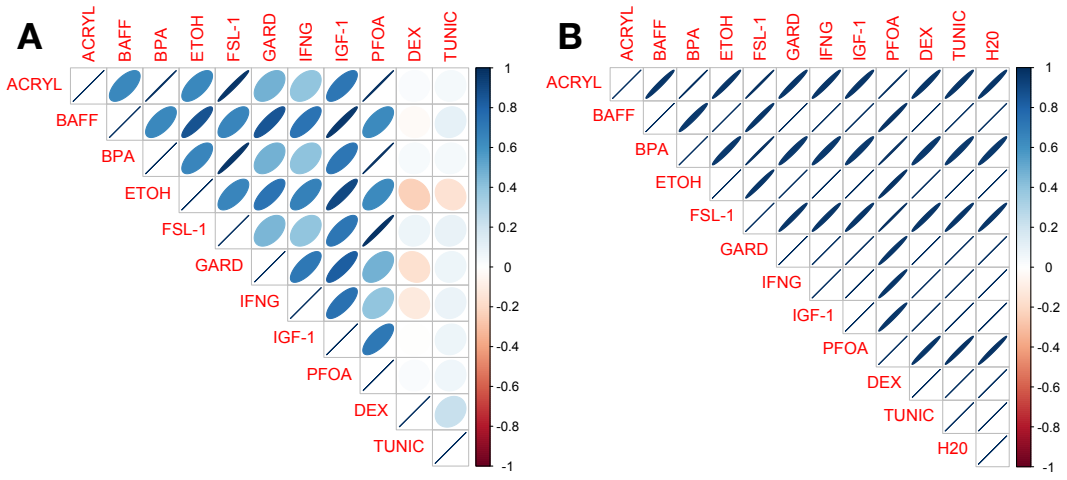

Figure S3. Phenotypic differentiation in gene expression (P_{ST}) versus genetic differentiation (F_{ST}) for African versus European samples. Plots show the distribution of P_{ST} values for: 1) AA genes identified in a given cellular environment (blue) and 2) a same-sized set of randomly selected genes (grey). The mean genome-wide F_{ST} value comparing genetic divergence between African and European samples is noted on the x-axis with an arrow. We find that all AA genes exhibit $P_{ST} > F_{ST}$ in all cellular environments, indicative of diversifying selection (Lamy et al. 2012; Leinonen et al. 2013).

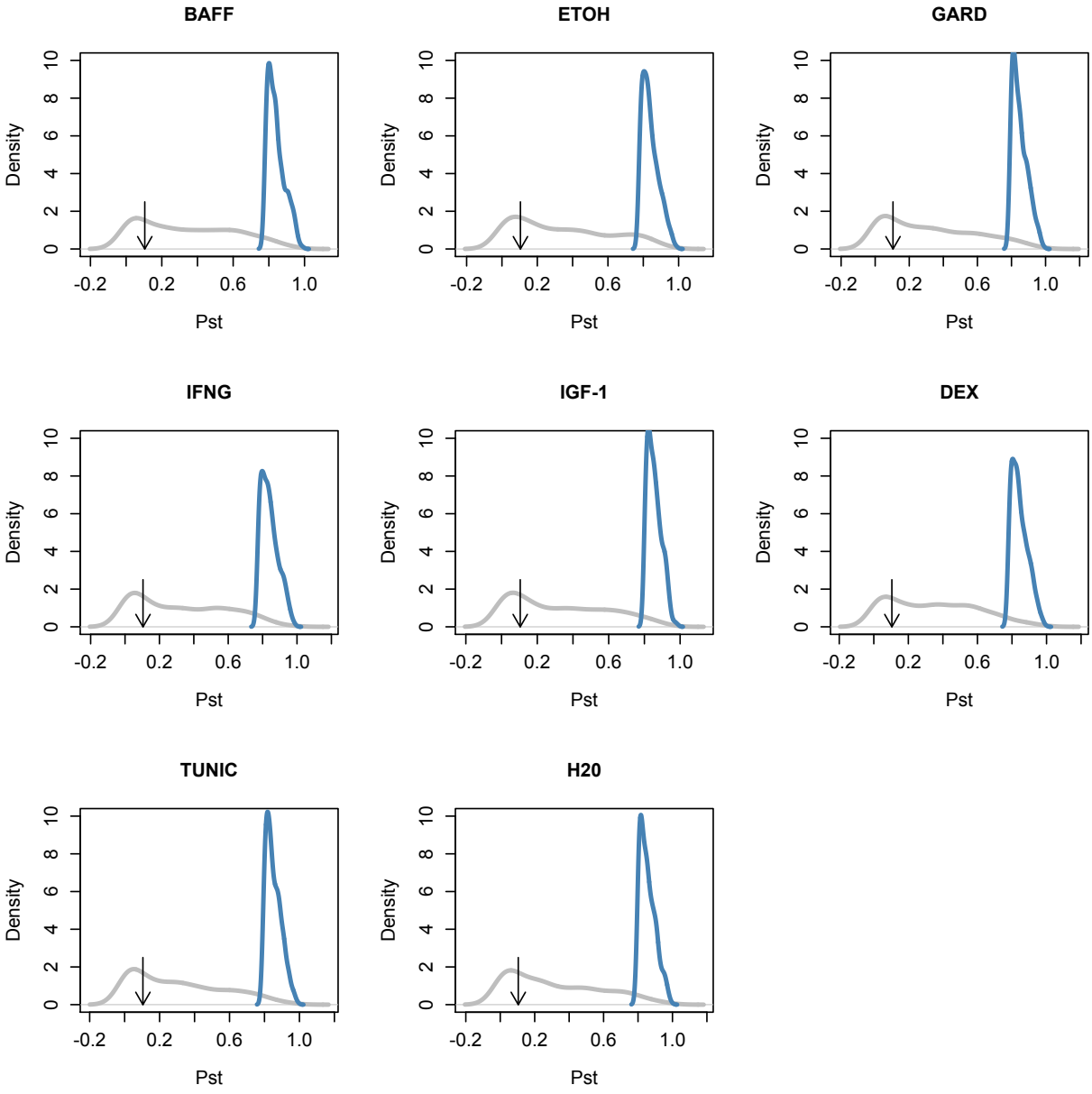

Figure S4. Enrichment of context-dependent and ubiquitous eQTL in particular chromatin states. X-axis shows the odds ratio from a Fisher's exact test asking whether ubiquitous or context-dependent eQTL were enriched in particular chromatin states relative to all SNPs tested as putative eQTL. Error bars represent 95% confidence intervals and chromatin state names on the y-axis are those defined by ENCODE (The ENCODE Project Consortium 2012).

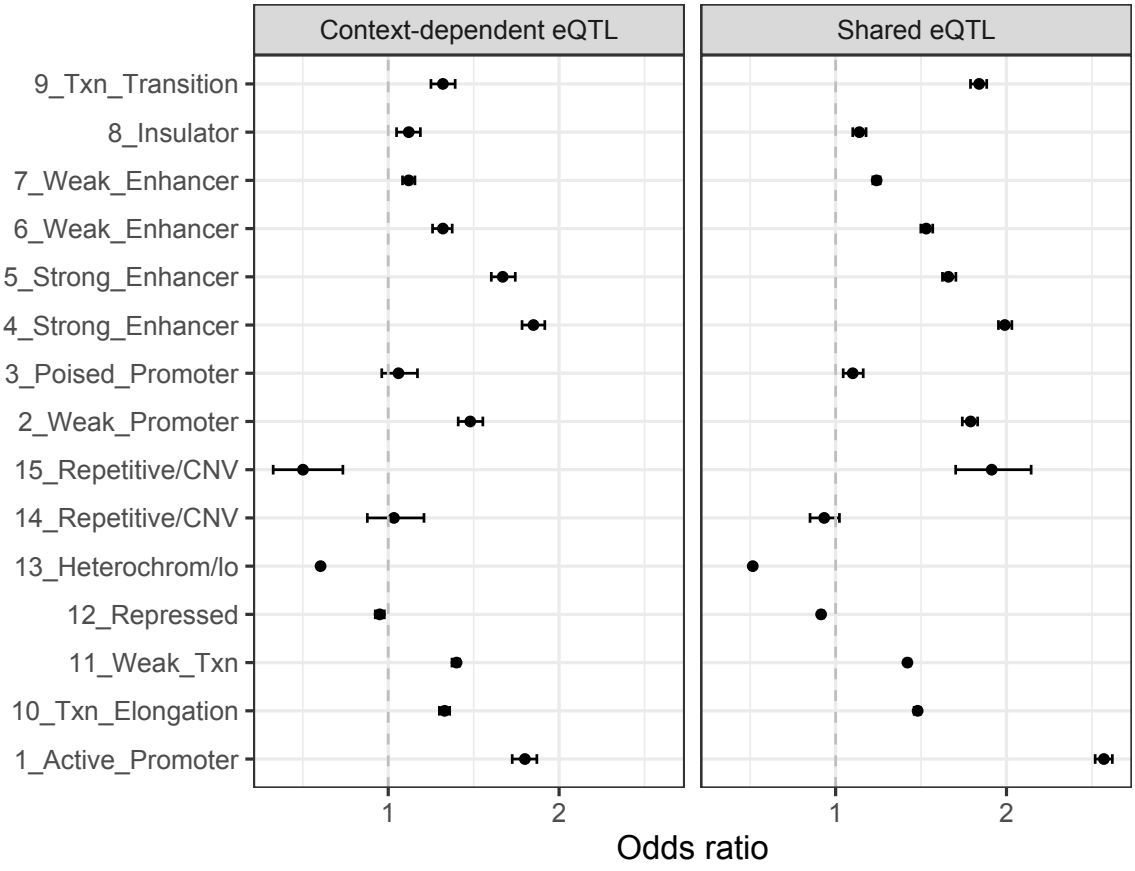

Figure S5. Read mapping does not systematically differ as a function of ancestry. Plot shows the proportion of reads that uniquely map (relative to the total number of reads generated) for all samples within one of our sequencing batches (n=1344 samples). Data are stratified by population and abbreviations were assigned by the 1000 Genomes Project as follows: GBR=British from England and Scotland; ESN=Esan in Nigeria; FIN=Finnish in Finland; GWD=Gambian in Western Division, Mandinka; IBS=Iberian populations in Spain; LWK=Luhya in Webuye, Kenya; MSL=Mende in Sierra Leone; TSI=Toscani in Italy; YRI=Yoruba in Ibadan, Nigeria; CEU=Utah residents with Northern and Western European ancestry from the CEPH collection. Colors indicate populations of European versus African ancestry. Using the CEU population as the reference, we found that only GWD had a significantly lower mapping rate (linear model, beta=-1.96, p=0.0073).

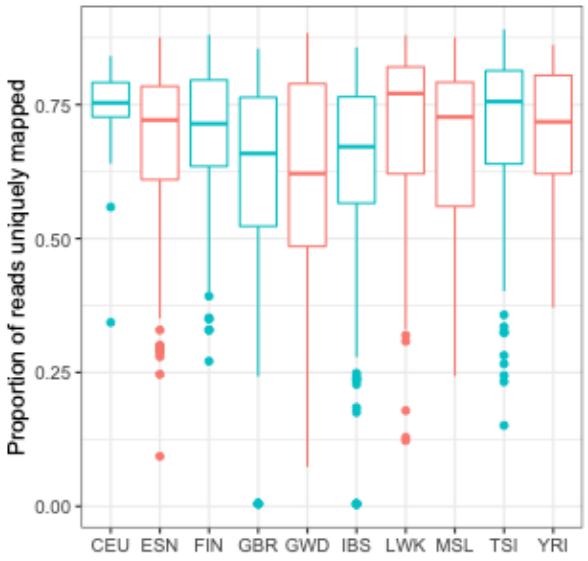

Figure S6. Principal components analyses reveal treatment and ancestry effects. We performed principal components analysis on the full, filtrered gene expression dataset (after surrogate variables were regressed out to remove technical effects). Top panels show the p-value from an analysis of variance testing for (A) treatment or (B) ancestry (African (AFR) versus European (EUR)) effects on the top 20 principal components (PCs). The dashed red line represents a nominal p-value of 0.05. Relationship between (C) treatment or (D) ancestry and principal component loadings for the PCs that were more strongly correlated with a given predictor variable.

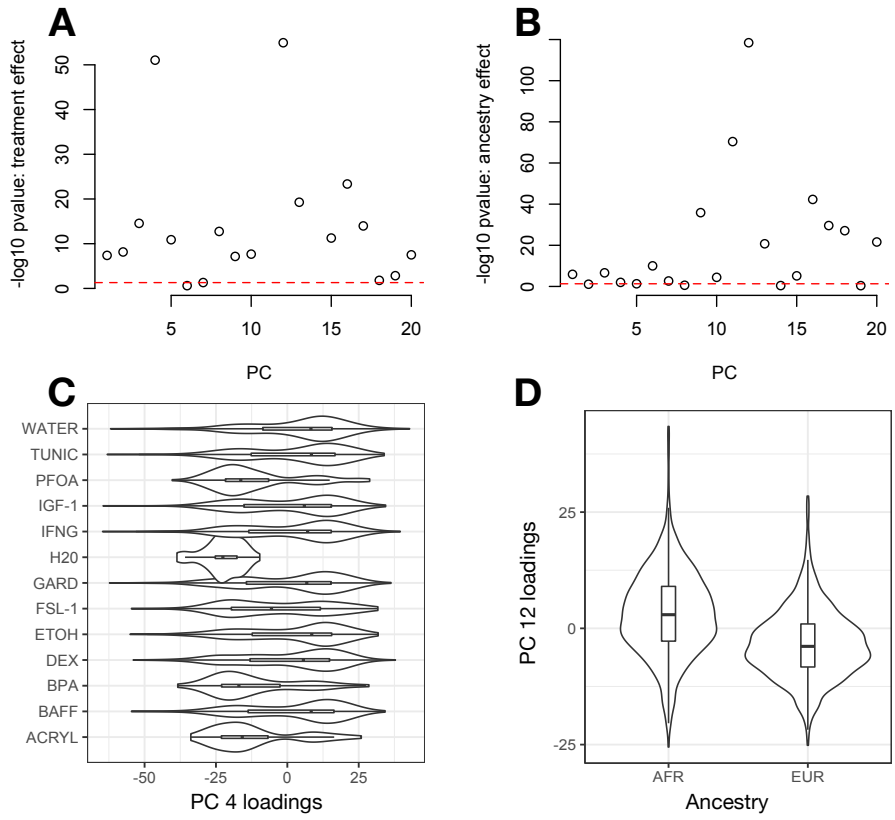

Figure S7. Overview of main analysis pipeline for identifying treatment (green), ancestry (red), and genetic (blue) effects on gene expression. Using this workflow, we assigned treatment, ancestry, and genetic effects to the following categories: 1) "ubiquitous", where a significant effect was shared across all treatments or environments; 2) "context-dependent", where a significant effect was not shared across all treatments or environments, and 3) a subset of context-dependent termed "condition-specific", where the effect was specific to one treatment or environment.

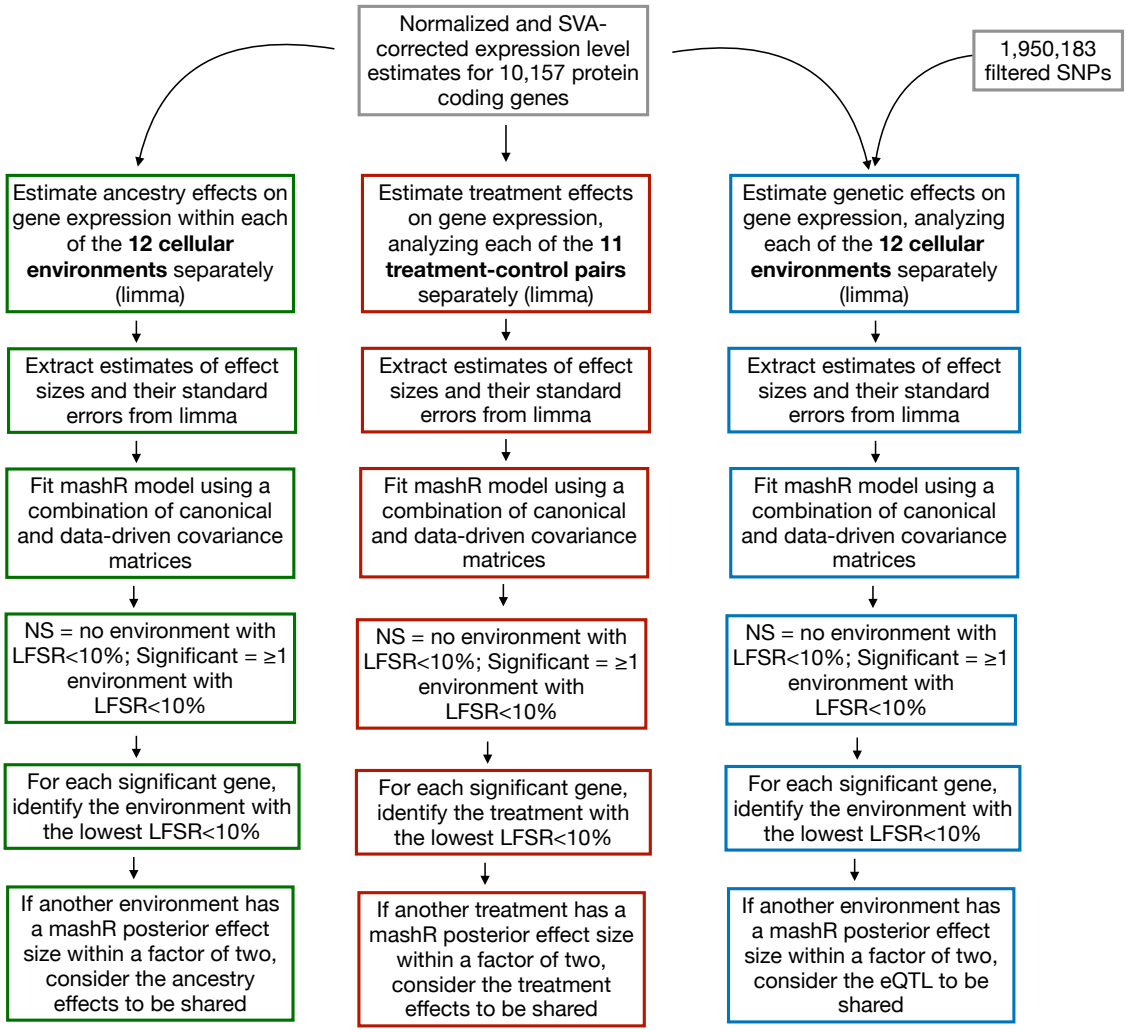

Figure S8. Sharing of treatment and ancestry effects after down sampling. To understand the impact of variable sample sizes across environments on our conclusions, we repeated the (A) treatment and (B) ancestry analyses described in the main text and overviewed in Figure S7 after randomly down sampling our data to n=120 per environment. We performed this subsampling five times and plotted the number of genes with shared treatment or ancestry effects in each analysis. Results are qualitatively similar to what is reported in the main text: most genes (82.4 ± 4.7%) have shared responses to only a handful of treatments (≤4); in contrast, almost all genes (97.4% ± 2.26%) have consistent ancestry effect across ≥8 environments.

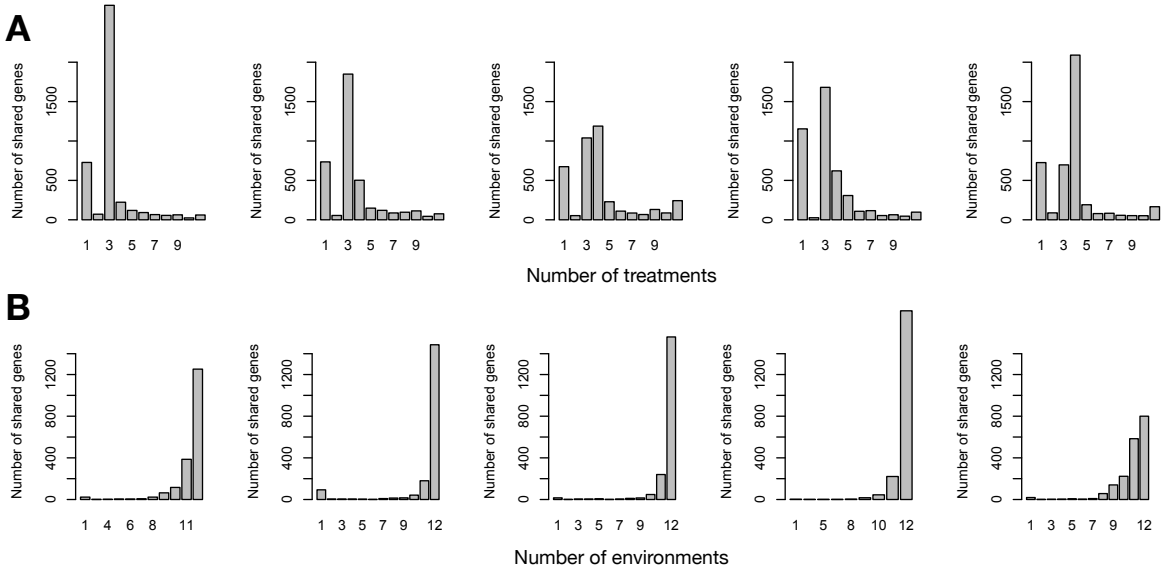

Figure S9. **Log fold expression changes in response to Dexamethasone are similar in this study relative to previous work**. Scatterplot was created with the R function "smoothScatter" using default parameters, and shows the correlation between the estimated log-fold changes estimated in previous work (Moyerbrailean et al. 2016) relative to this study. All genes that passed filters in both datasets are shown (n=10,032 genes).

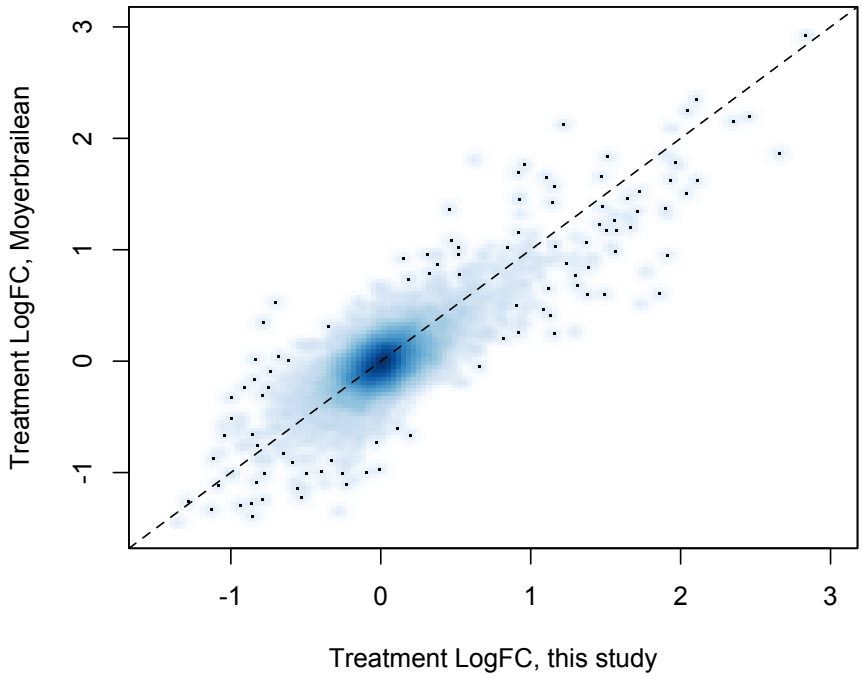

Figure S10. Differentially expressed (DE) genes shared between environments. (A) In Figure 1C, we present a version of panel A that shows that many genes are environment specific, few genes have similar effect sizes in 2 environments, and many genes have effect sizes that are similar across 3 or more environments. This result is driven by a large number of DEX-specific genes. Here we show the same distribution as plotted in Figure 1C, but with DEX excluded from the dataset. (B) For each environment, the number of genes included in the N=3 bar in Figure 1C is plotted. In combination with Figure 1D, this result emphasizes that many genes in our dataset have similar DE effect sizes shared across the group of 3 environmental contaminants (ACRYL, BPA, PFOA), or shared across some subset of a group of hormonal and immune treatments (GARD, IFNG, BAFF, IGF1).

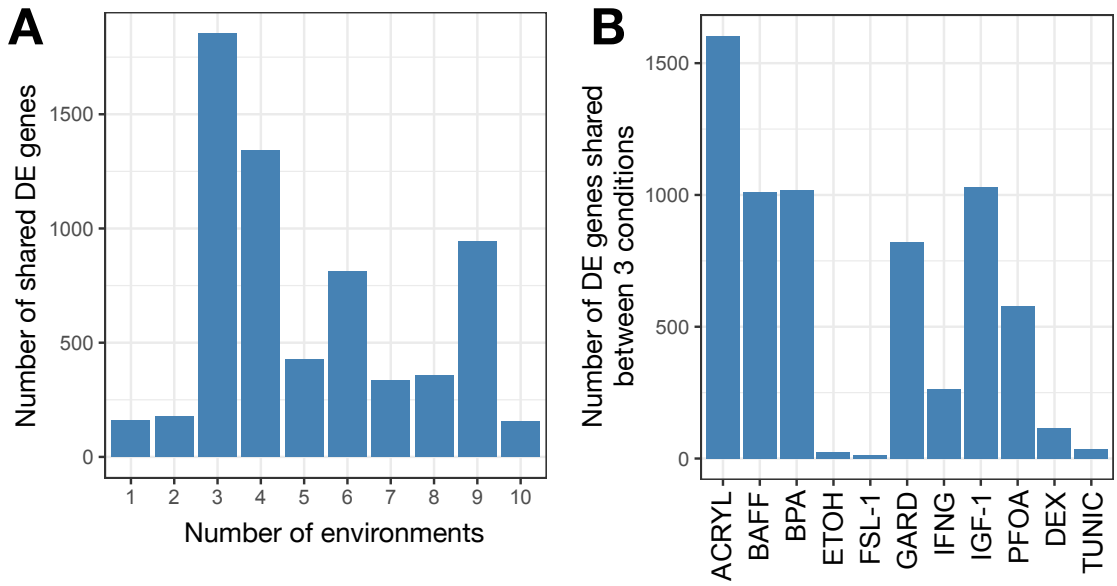

SUPPLEMENTARY REFERENCES

Aguet F, Brown AA, Castel SE, Davis JR, He Y, Jo B, Mohammadi P, Park Y, Parsana P, Segrè A V, et al. 2017. Genetic effects on gene expression across human tissues. *Nature* **550**: 204–213. https://doi.org/10.1038/nature24277.

Anders S. 2011. HTSeq: Analysing high-throughput sequencing data with Python. http://www-huber.embl.de/users/anders/HTSeq/.

Banovich NE, Li YI, Raj A, Ward MC, Greenside P, Calderon D, Tung PY, Burnett JE, Myrthil M, Thomas SM, et al. 2018. Impact of regulatory variation across human iPSCs and differentiated cells. *Genome Res* **28**: 122–131.

Byrska-Bishop M, Evani US, Zhao X, Basile AO, Abel HJ, Regier AA, Corvelo A, Clarke WE, Musunuri R, Nagulapalli K, et al. 2021. High coverage whole genome sequencing of the expanded 1000 Genomes Project cohort including 602 trios. *bioRxiv*. https://www.biorxiv.org/content/early/2021/02/07/2021.02.06.430068.

Casañas-Sánchez V, Pérez JA, Quinto-Alemany D, Díaz M. 2016. Sub-toxic Ethanol Exposure Modulates Gene Expression and Enzyme Activity of Antioxidant Systems to Provide Neuroprotection in Hippocampal HT22 Cells. *Front Physiol* **7**. https://www.frontiersin.org/articles/10.3389/fphys.2016.00312.

Dobin A, Davis CA, Schlesinger F, Drenkow J, Zaleski C, Jha S, Batut P, Chaisson M, Gingeras TR. 2013. STAR: ultrafast universal RNA-seq aligner. *Bioinformatics* 1–7.

Findley AS, Monziani A, Richards AL, Rhodes K, Ward MC, Kalita CA, Alazizi A, Pazokitoroudi A, Sankararaman S, Wen X, et al. 2021. Functional dynamic genetic effects on gene regulation are specific to particular cell types and environmental conditions ed. S.C.J. Parker. *Elife* **10**: e67077. https://doi.org/10.7554/eLife.67077.

Hindorff LA, Sethupathy P, Junkins HA, Ramos EM, Mehta JP, Collins FS, Manolio TA. 2009. Potential etiologic and functional implications of genome-wide association loci for human diseases and traits. *Proc Natl Acad Sci* **106**: 9362 LP – 9367. http://www.pnas.org/content/106/23/9362.abstract.

Karolchik D, Barber GP, Casper J, Clawson H, Cline MS, Diekhans M, Dreszer TR, Fujita P a., Guruvadoo L, Haeussler M, et al. 2014. The UCSC Genome Browser database: 2014 update. *Nucleic Acids Res* **42**: 764–770.

Lamy J-B, Plomion C, Kremer A, Delzon S. 2012. QST < FST as a signature of canalization. *Mol Ecol* **21**: 5646–5655. https://doi.org/10.1111/mec.12017.

Law CW, Chen Y, Shi W, Smyth GK. 2014. Voom! Precision weights unlock linear model analysis tools for RNA-seq read counts. *Genome Biol* **15**: R29.

Leek JT, Storey JD. 2009. Capturing heterogeneity in gene expression studies by surrogate variable analysis. *PLoS Genet* **3**: e161.

Leinonen T, McCairns RJS, O'Hara RB, Merilä J. 2013. QST–FST comparisons: evolutionary and ecological insights from genomic heterogeneity. *Nat Rev Genet* **14**: 179–190. https://doi.org/10.1038/nrg3395.

Lek M, Karczewski KJ, Minikel E V, Samocha KE, Banks E, Fennell T, O'Donnell-Luria AH, Ware JS, Hill AJ, Cummings BB, et al. 2016. Analysis of protein-coding genetic variation in 60,706 humans. *Nature* **536**: 285–291. https://doi.org/10.1038/nature19057.

Martin M. 2011. Cutadapt removes adapter sequences from high-throughput sequencing reads. *EMBnet.journal* **17**: 10–12.

http://journal.embnet.org/index.php/embnetjournal/article/view/200.
Moyerbrailean GA, Richards AL, Kurtz D, Kalita CA, Davis GO, Harvey CT, Alazizi A, Watza D, Sorokin Y, Hauff N, et al. 2016. High-throughput allele-specific expression across 250 environmental conditions. *Genome Res* **26**: 1627–1638.
Nguyen S, Nguyen H, Truong K. 2020. Comparative cytotoxic effects of methanol, ethanol and DMSO on human cancer cell lines. *Biomed Res Ther* **7**. http://home.biomedpress.org/index.php/BMRAT/article/view/614.
Pallares LF, Picard S, Ayroles JF. 2020. TM3'seq: A Tagmentation-Mediated 3' Sequencing Approach for Improving Scalability of RNAseq Experiments. *G3 Genes, Genomes, Genet* **10**: 143–150. https://www.g3journal.org/content/10/1/143.
Purcell S, Neale B, Todd-Brown K, Thomas L, Ferreira MAR, Bender D, Maller J, Sklar P, de Bakker PIW, Daly MJ, et al. 2007. PLINK: a tool set for whole-genome association and population-based linkage analyses. *Am J Hum Genet* **81**: 559–575. https://pubmed.ncbi.nlm.nih.gov/17701901.
Quinlan AR, Hall IM. 2010. BEDTools: A flexible suite of utilities for comparing genomic features. *Bioinformatics* **26**: 841–842.
Rashid M, Coombs KM. 2019. Serum-reduced media impacts on cell viability and protein expression in human lung epithelial cells. *J Cell Physiol* **234**: 7718–7724. https://doi.org/10.1002/jcp.27890.
Šarc L, Lipnik-Štangelj M. 2009. Comparison of Ethanol and Acetaldehyde Toxicity in Rat Astrocytes in Primary Culture. *Arch Ind Hyg Toxicol* **60**: 297–305. https://doi.org/10.2478/10004-1254-60-2009-1927.
Storey JD, Tibshirani R. 2003. Statistical significance for genomewide studies. *Proc Natl Acad Sci U S A* **100**: 9440–9445. http://www.pubmedcentral.nih.gov/articlerender.fcgi?artid=170937&tool=pmcentrez&rendertype=abstract.
Subramanian A, Tamayo P, Mootha VK, Mukherjee S, Ebert BL, Gillette MA, Paulovich A, Pomeroy SL, Golub TR, Lander ES, et al. 2005. Gene set enrichment analysis: A knowledge-based approach for interpreting genome-wide expression profiles. *Proc Natl Acad Sci* **102**: 15545–15550. https://www.pnas.org/content/102/43/15545.
The 1000 Genomes Project Consortium. 2012. An integrated map of genetic variation from 1,092 human genomes. *Nature* **135**: 0–9.
The ENCODE Project Consortium. 2012. An integrated encyclopedia of DNA elements in the human genome. *Nature* **489**: 57–74. http://www.nature.com/doifinder/10.1038/nature11247.
Tuoi Do TH, Gaboriau F, Ropert M, Moirand R, Cannie I, Brissot P, Loréal O, Lescoat G. 2011. Ethanol Effect on Cell Proliferation in the Human Hepatoma HepaRG Cell Line: Relationship With Iron Metabolism. *Alcohol Clin Exp Res* **35**: 408–419. https://doi.org/10.1111/j.1530-0277.2010.01358.x.
Urbut SM, Wang G, Carbonetto P, Stephens M. 2019. Flexible statistical methods for estimating and testing effects in genomic studies with multiple conditions. *Nat Genet* **51**: 187–195. https://doi.org/10.1038/s41588-018-0268-8.
Visscher PM, Hemani G, Vinkhuyzen AAE, Chen G-B, Lee SH, Wray NR, Goddard ME, Yang J. 2014. Statistical Power to Detect Genetic (Co)Variance of Complex Traits Using SNP Data in Unrelated Samples. *PLOS Genet* **10**: e1004269. https://doi.org/10.1371/journal.pgen.1004269.
Yang J, Lee SH, Goddard ME, Visscher PM. 2011. GCTA: A tool for genome-wide complex

trait analysis. *Am J Hum Genet* **88**: 76–82. http://dx.doi.org/10.1016/j.ajhg.2010.11.011.
Zhang Y, Quick C, Yu K, Barbeira A, Luca F, Pique-Regi R, Kyung Im H, Wen X, Consortium TGte. 2020. PTWAS: investigating tissue-relevant causal molecular mechanisms of complex traits using probabilistic TWAS analysis. *Genome Biol* **21**: 232. https://doi.org/10.1186/s13059-020-02026-y.
Zheng X, Baker H, Hancock WS, Fawaz F, McCaman M, Pungor Jr. E. 2006. Proteomic Analysis for the Assessment of Different Lots of Fetal Bovine Serum as a Raw Material for Cell Culture. Part IV. Application of Proteomics to the Manufacture of Biological Drugs. *Biotechnol Prog* **22**: 1294–1300. https://doi.org/10.1021/bp060121o.